Chemical ordering of FePt nanoparticles by pulsed laser annealing

2004 J. Phys.: Condens. Matter 16 6385

(http://iopscience.iop.org/0953-8984/16/36/005)

INSTITUTE OF PHYSICS PUBLISHING JOURNAL OF PHYSICS: CONDENSED MATTER

J. Phys.: Condens. Matter **16** (2004) 6385–6394 PII: S0953-8984(04)76350-X

Chemical ordering of FePt nanoparticles by pulsed laser annealing

Soichiro Saita[1] **and Shinya Maenosono**[2,3]

[1] Mitsubishi Chemical Group Science and Technology Research Centre, Incorporated, Kamoshida-cho, Aoba-ku, Yokohama, Kanagawa 227-8502, Japan
[2] Department of Chemical System Engineering, University of Tokyo, Hongo 7-3-1, Bunkyo-ku, Tokyo 113-8656, Japan

E-mail: shinya@chemsys.t.u-tokyo.ac.jp

Received 16 February 2004
Published 27 August 2004
Online at stacks.iop.org/JPhysCM/16/6385
doi:10.1088/0953-8984/16/36/005

Abstract

An irradiation with the third-harmonic wave of a Nd:yttrium–aluminium–garnet (YAG) laser with a 5 ns pulse width successfully transformed colloid–chemically synthesized FePt nanoparticles (NPs) from disordered face-centred cubic (fcc) into chemically ordered $L1_0$ (face-centred tetragonal: fct) phase. Granular films and hexane dispersions of fcc-FePt NPs were irradiated by the pulsed laser beam. In the case of the granular film, a coercivity of 1 kOe was achieved after the laser irradiation; meanwhile, the dispersion sample exhibited superparamagnetism, although the crystalline structure was transformed into fct phase. X-ray diffractometry and transmission electron microscopy revealed that coalescence between NPs was fairly well suppressed in the case of the dispersion sample. The superparamagnetism observed in the dispersion sample was due to insignificant coalescence and the resulting small magnetic domain.

1. Introduction

The area density of magnetic storage media increases with each passing year and researchers have aimed at the realization of the density of Tbit in^{-2}. Nano-sized magnetic materials have attracted attention and have been intensively investigated for this purpose. In general, ferromagnetic materials lose their ferromagnetism under a certain critical size. This is due to the disordering of magnetic moments becoming prominent, which is caused by thermal disturbance (superparamagnetism) [1, 2]. $L1_0$-phase FePt has large uniaxial magnetic anisotropy and shows ferromagnetism at room temperature even if the domain size is smaller than 10 nm. It is thus expected to be a good candidate for ultra-high density magnetic storage media [3–8].

[3] Author to whom any correspondence should be addressed.

Recently, a colloid–chemical synthesis technique of FePt nanoparticles (NPs) has been developed and the FePt NPs are regarded as one of the most likely candidates for ultra-high density nano-sized magnetic materials [3–6, 8]. The colloid–chemically synthesized FePt NPs have chemically disordered fcc structure in which Fe and Pt atoms are randomly arranged and are superparamagnetic. Post-synthesis thermal annealing at a temperature over 580 °C transforms the crystalline structure from face-centred cubic (fcc) to $L1_0$ (face-centred tetragonal: fct). Using a furnace, the FePt NPs are normally annealed in the form of a close-packed granular film deposited on a solid substrate. This usually causes severe coalescence of NPs and makes the size distribution of NPs larger. To avoid the undesirable coalescence of NPs, several attempts have been proposed, for example, lowering the transition temperature by adding impurities such as Ag [9], or by stabilizing NPs on the substrate coated with highly coordinating molecules [10].

However, the preparation of isolated monodisperse fct-FePt NPs is, in principle, difficult using the aforementioned annealing methods. If one could obtain isolated monodisperse fct-FePt NPs in liquid, it is expected not only to solve the problem of coalescence during the annealing, but also to utilize the fct-FePt NPs for other applications, such as biological immunoassay [11], magnetofection [12] or ferromagnetic nanocomposite [13]. A new synthetic approach has recently been proposed to directly obtain fct-FePt NPs [8, 14].

Pulsed-laser annealing enables materials to be heated to very high temperatures in an extremely short period of time (100 fs–100 ns), preventing heat diffusion. Thus, one can precisely anneal a selected area of material [15]. Due to many advantages over conventional annealing techniques, laser annealing has been utilized for decades in many fields. For example, Brotherton and co-workers [16] used an excimer laser to crystallize a-Si on a glass substrate. Pulsed-laser annealing [17] or abrasion [18, 19] of NPs in various matrices has been reported recently. Koda and co-workers found that the size of Au NPs in water was affected by irradiation of the second-harmonic wave of a Nd:YAG laser (pulse width 7 ns, power 800 mJ cm^{-2}) [18]. Kamat and co-workers also found that the melting and coalescence of Au NPs occurred with irradiation of the second-harmonic wave of a Nd:YAG laser (pulse width 18 ps, power 15 mJ $pulse^{-1}$) [19].

In this paper, we report the first attempt of pulsed-laser annealing to obtain fct-FePt NPs without severe coalescence by irradiation of the third-harmonic wave of a Nd:YAG laser with a 5 ns pulse width. Granular films and hexane dispersions of fcc-FePt NPs were irradiated by the pulsed laser beam. To evaluate the effects of laser irradiation, crystalline structures were investigated by x-ray diffractometry (XRD), transmission electron microscopy (TEM) and selected area electron diffraction (SAED). Magnetizing properties were investigated by vibrating sample magnetometry (VSM).

2. Experimental details

2.1. UV–vis spectroscopy

The absorption spectrum of FePt NPs was obtained by UV–vis spectrophotometer (Hewlett-Packard, HP8453) in the range of 200–1000 nm. A 1.5 ml sample of NP/hexane dispersion (0.03 wt% solid concentration) was placed in a quartz cuvette in a holder of the spectrophotometer for absorption spectrum measurement.

2.2. Structural characterization

XRD patterns of FePt NPs were obtained in the reflection geometry by x-ray diffractometer (Rigaku, RINT200PC) at room temperature, using Cu Kα radiation (wavelength 1.542 Å,

incident angle 1°, step width 0.05°, counting time 1 s). FePt NPs were deposited on glass substrates (Matsunami Micro Slide Glass, 8×10 mm^2) by casting and drying the NP/hexane dispersion for XRD measurements. High-resolution TEM micrographs and selected area electron diffraction (SAED) patterns of FePt NPs were obtained using a Hitachi H-9000UHR microscope operated at 300 kV.

2.3. Vibrating sample magnetometer

Magnetization curves of FePt NPs were obtained by using VSM (RikenDenshi, BHV-50). In-plane measurements were performed at room temperature. The maximum applied field and frequency were 15 kOe and 28 Hz, respectively. FePt NPs were deposited on glass substrates by casting and drying the NP/hexane dispersion several times for magnetic measurements.

2.4. FePt nanoparticle synthesis

FePt NPs were synthesized by conventional colloid–chemical methods [3–6, 8]. Platinum diacetylacetonate ($Pt(acac)_2$, purity 97%), 1,2-hexanediol (98%), octyl ether (99%), oleic acid (90%) and oleylamine (70%) were purchased from Aldrich. Iron pentacarbonyl ($Fe(CO)_5$, 95%) was purchased from Kanto Kagaku. The reaction temperature was maintained at 286 °C. The synthesis was based on the thermal decomposition of $Fe(CO)_5$ and the reduction of $Pt(acac)_2$, which took place simultaneously in the reaction followed by the nucleation and growth of FePt NPs. The molar ratio of Fe to Pt was adjusted to 2:1, taking into consideration the evaporation of $Fe(CO)_5$ when the reaction temperature rose higher than its boiling point. The hexane dispersion of FePt NPs capped with oleic acid (1.5 wt% solid concentration) was obtained by this process. The composition of FePt NPs was determined to be $Fe_{58}Pt_{42}$ by inductively coupled plasma atomic emission spectrometry (ICP-AES; Jobin Yvon, JY38S).

2.5. Furnace annealing

A conventional thermal annealing experiment in a furnace was carried out to compare to laser annealing. As-synthesized FePt NPs were deposited on a glass substrate by casting and drying the NP/hexane dispersion several times. A uniform film of obtained FePt NPs was put in an electric furnace and annealed at 600 °C for 30 min in Ar/H_2 (3/2) reduction atmosphere. The term 'furnace annealing' will be abbreviated as 'FA' hereafter.

2.6. Laser annealing

A Q-switched Nd:YAG laser (Quantel, Brilliant) was used for laser annealing experiments. The pulse width, wavelength, frequency and power were 5 ns, 355 nm, 10 Hz and 40–1000 mW cm^{-2}, respectively. Figure 1 shows a schematic illustration of an experimental set-up. A granular film (FePt film) and hexane dispersions (FePt dispersion) of as-synthesized FePt NPs were irradiated by the pulsed laser beam. The FePt film was fabricated in the same way as described in the section on furnace annealing. The FePt film was irradiated with a 2 mm spot laser (solid-phase laser annealing: SPLA). In this case, laser irradiation longer than 1 s caused sublimation of the FePt NPs. Thus, the laser spot was manually scanned in such a way that an average holding time of the spot was 0.5 s at the same position on the FePt film. The laser annealing of FePt dispersion (liquid-phase laser annealing: LPLA) was performed under the following two conditions: (a) lateral irradiation of an unstirred FePt dispersion (0.08 wt% concentration, clear light brown) with a 2 cm spot beam in a quartz cell ($1 \times 1 \times 4.5$ cm^3) for 36 s (2 cm spot LPLA), and (b) irradiation of the stirred FePt dispersion (1.5 wt% concentration,

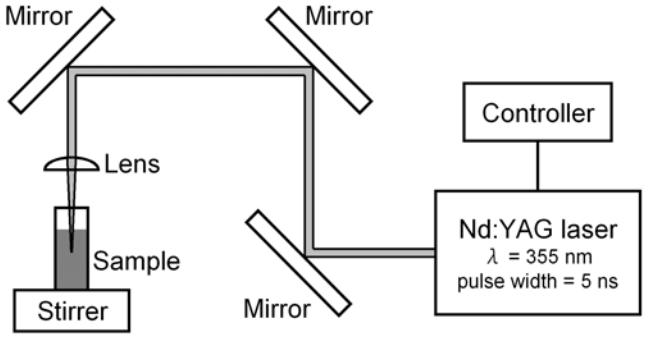

Figure 1. Schematic illustration of an experimental set-up in the case of 1 mm spot LPLA.

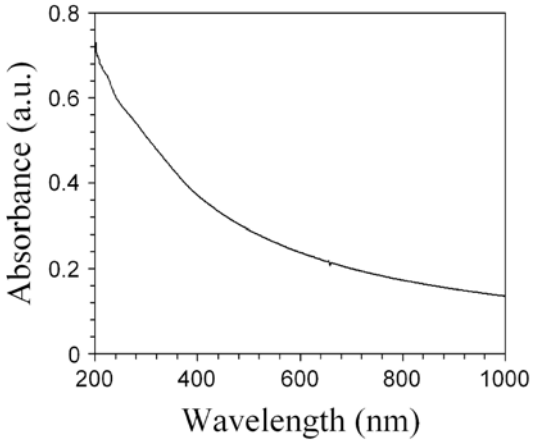

Figure 2. Absorption spectrum of as-synthesized FePt NPs dispersed in hexane (0.03 wt%).

inky black) with a 1 mm spot beam from above in the quartz cell for 2.5 h (1 mm spot LPLA) as shown in figure 1.

3. Results and discussion

Figure 2 shows the absorption spectrum of as-synthesized FePt NPs. Absorption is seen in the range from UV to near IR and, notably, is more significant at shorter wavelength. Hence, the laser light used in our experiments was considered to be well absorbed by the NPs.

Figure 3(a) shows the XRD pattern of as-synthesized FePt NPs. Characteristic broad peaks of fcc-FePt NPs [3, 10, 20, 21] are seen. Figure 3(b) shows the XRD pattern of the sample annealed in the furnace. The superlattice reflections (001) and (110) appeared and an increase in the angle of the (111) peak was observed. In addition, (200), (002) and (210) peaks could be clearly seen, indicating that the crystalline structure was successfully transformed into fct by FA. The half-maximum full width of the (111) peak of figure 3(b) is much smaller than that of figure 3(a). This suggests that coalescence of the NPs [9, 22, 23] proceeded during annealing and the crystalline size increased. The peak positions of the annealed sample were consistent with the reported result [3].

The XRD patterns of laser annealed samples are shown in figure 4. Curves (a) and (b) correspond to the XRD patterns of as-synthesized and SPLA samples, respectively. Note

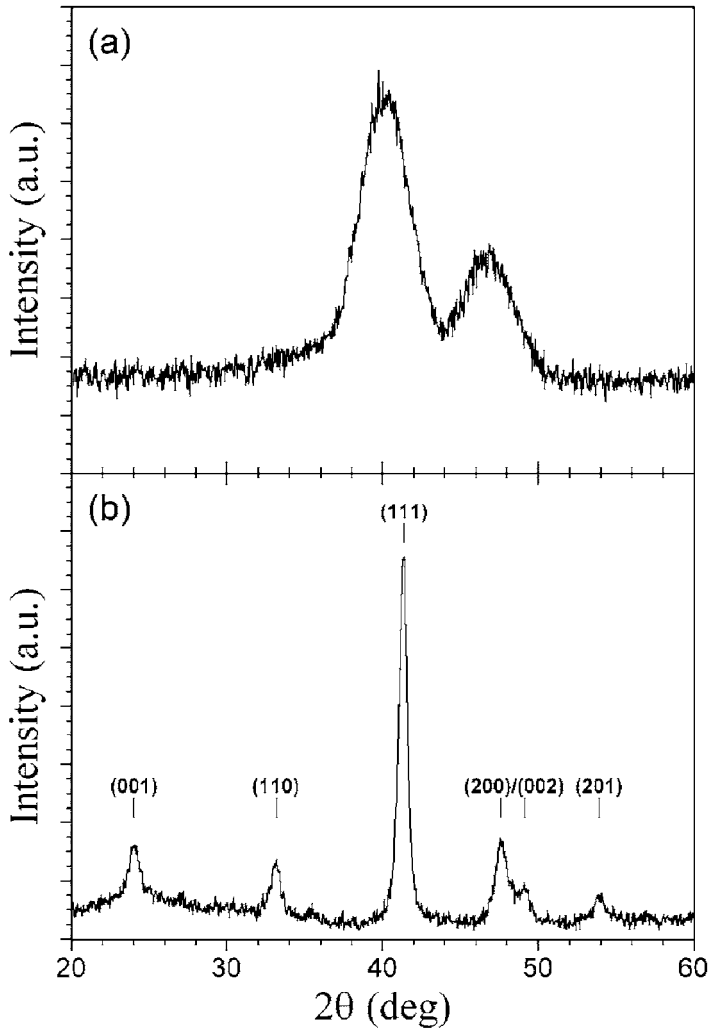

Figure 3. X-ray diffraction patterns of (a) as-synthesized FePt NPs and (b) FePt NPs annealed in the furnace.

that (a) is the same as figure 3(a). In the case of the SPLA sample, the XRD pattern looks identical with that of the as-synthesized NPs. However, the single-Gaussian fit of the (111) peak was ill fitted to the experimental data of the SPLA sample (curve (b)), whereas a single Gauss function coincided with the (111) peak of the as-synthesized FePt NPs (curve (a)). This suggests that fct-NPs were partly generated in SPLA and the reflections from fct phase overlapped with those of fcc-NPs. Since the peak of the XRD pattern of the SPLA sample was not separable, the degree of coalescence was unclear.

Curve (c) is the XRD pattern of the 2 cm spot LPLA sample. In this case, a halo-like peak seen at 20°–35° could be due to the reflection from amorphous carbon [24]. On the other hand, both (111) and (200) peaks were identical to those of as-synthesized fcc-NPs (curve (a)), in contrast to the case of SPLA. These results imply that the laser irradiation caused an increase in temperature of the NPs which resulted in carbonizing oleic acid on the surfaces

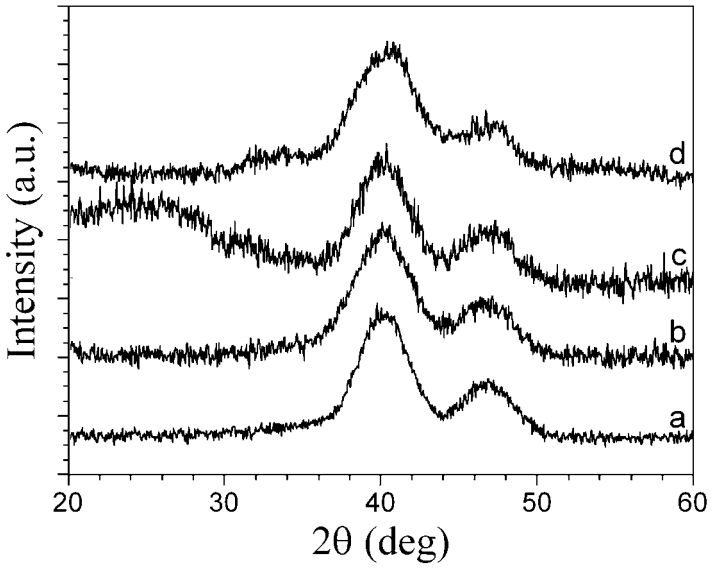

Figure 4. X-ray diffraction patterns of (a) as-synthesized, (b) SPLA, (c) 2 cm spot LPLA and (d) 1 mm spot LPLA samples.

without phase transition. There are two possible interpretations to elucidate the lack of phase transition: (1) the temperature rise is insufficient to promote phase transition, and (2) although the temperature rise is well over the transition, the irradiation time is insufficient due to rapid quenching. However, we could rule out the second possibility because no significant variation in the XRD pattern was observed when the irradiation time was varied in the range of 36–3600 s (data not shown).

Consequently, we can conclude that the temperature rise was insufficient for phase transition in the case of the 2 cm spot LPLA. Nonetheless, the average temperature of NPs should be 250–580 °C, because the temperature required for carbonization of oleic acid to amorphous carbon is 250–400 °C [25]. Neither precipitation nor turbidity was observed by visual inspection in the NP dispersion after the laser irradiation.

Curve (d) shows the XRD pattern of the 1 mm spot LPLA sample. One can see the superlattice reflection (110) clearly appeared while the (001) superlattice peak was absent. Additionally, the (111) and (200) peaks slightly shifted toward larger angles. These experimental facts are consistent with the previous results of phase transition of ultra-small FePt NPs [10, 21]. In some cases, ultra-small FePt NPs exhibit ferromagnetism even though the (110) superlattice peak, which was observed in our case, is absent. Also note that no halo-like peak at lower angle was observed.

To analyse the XRD pattern in detail, the spectrum curve in the range $27° \leqslant 2\theta \leqslant 56°$ was deconvoluted by using five Gauss functions as shown by dashed curve peaks and numbers in figure 5. Peaks 1, 3 and 5 correspond to (110), (111) and (200) peaks of fct-NPs (figure 3(b)), respectively. Assuming the FA sample to be perfectly ordered, the long-range order parameter S was estimated for the 1 mm spot LPLA sample by the equation

$$S = \left(I_{110}^{\mathrm{LA}}/I_{111}^{\mathrm{LA}}\right) / \left(I_{110}^{\mathrm{FA}}/I_{111}^{\mathrm{FA}}\right), \tag{1}$$

where I_{110}^{LA} and I_{111}^{LA} are the intensities of the (110) and (111) peaks of the fct phase 1 mm spot LPLA sample, respectively (peaks 1 and 3 in figure 5). Moreover, I_{110}^{FA} and I_{111}^{FA} are the intensities of the (110) and (111) peaks of the FA sample (see figure 3(b)). As a result, S was

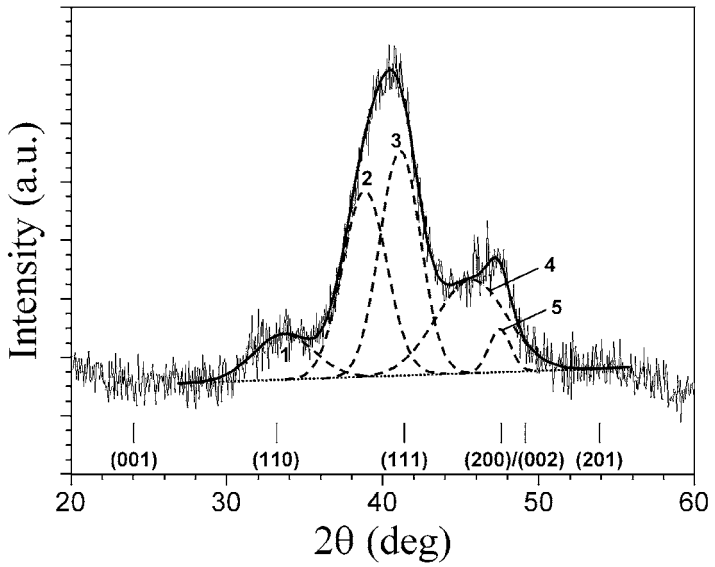

Figure 5. X-ray diffraction pattern of the 1 mm spot LPLA sample. Dashed curves represent the Gaussian deconvolutions of the peaks. The bold curve corresponds to the composition of all Gaussian curves. For comparison, peak positions of the FA sample are indicated below by bars.

approximately unity. These results indicate that some fcc-NPs were transformed into fct-NPs. In addition, the transformed fct-NPs have almost the same crystalline structure as the fct-NPs obtained by FA. Narrowing the laser spot to 1 mm efficiently elevated the NP temperature high enough to promote the transition in one pulse. The average crystalline sizes of fcc- and fct-NPs in the laser annealed sample were calculated by the Scherrer formula [26] using the half-maximum full width of peaks 2 and 3 in figure 5, and the results were 2.5 and 2.8 nm, respectively. With respect to the half-maximum full width of the (111) peak, the fitting result is close to the minimum value even if the number of Gaussian functions decreases from five to four or three; that is, the NP size estimated is the maximum value. The average size of crystallites of as-synthesized NPs was 2.2 nm.

The reason why the halo-like peak which was observed in the case of the 2 cm spot LPLA disappeared in curve (d) can be elucidated as follows. It is well known that carbon directly reacts with iron oxide as reducing agent at $>950\,^{\circ}$C. As a result, carbon itself is oxidized and transfers to CO_x. Thus, carbon produced on the NP surface in the course of laser annealing may be immediately consumed by the reaction with iron oxide at the surface. Alternatively, the reaction of carbon with dissolved oxygen in liquid [19] may also take place. However, the fact that the fct-phase peaks of the 1 mm spot LPLA sample coincided with those of the FA sample annealed in a reducing atmosphere supports the carbonization of oleic acid followed by the reduction of FePt NPs in the LPLA process. We observed no change in the NP dispersion by visual inspection after the long-period irradiation; that is, there was no macroscopic precipitate at the bottom of the sample.

Figures 6(a) and (b) show high-resolution TEM micrographs of the as-synthesized and 1 mm spot LPLA samples, respectively. The average diameter is estimated to be about 2 nm for both samples from the TEM micrographs. This result is consistent with the above-mentioned XRD analysis. Additionally, the SAED patterns of as-synthesized and 1 mm spot LPLA samples are shown in figures 6(a) and (b), respectively. The $L1_0$-phase FePt 110

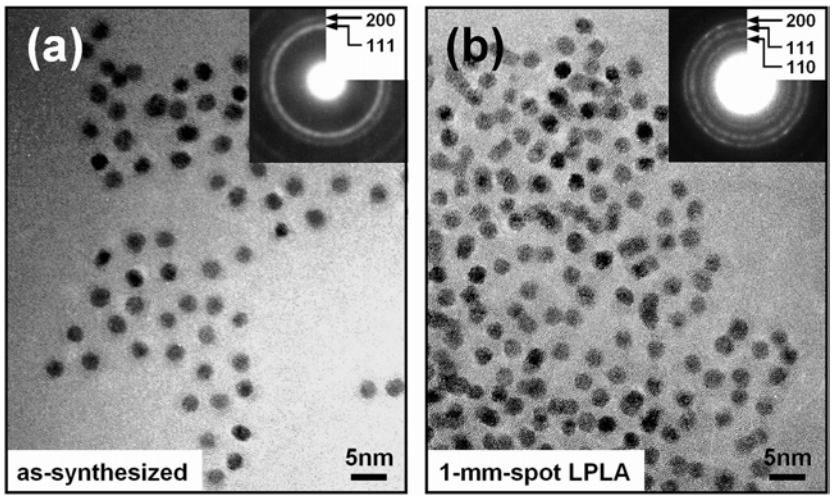

Figure 6. High-resolution TEM micrographs of (a) as-synthesized and (b) 1 mm spot LPLA samples. The insets above right in (a) and (b) represent the SAED patterns of respective samples.

superlattice reflections are clearly observed in the SAED pattern of the 1 mm spot LPLA sample (figure 6(b)), while they are absent in the SAED pattern of the as-synthesized sample (figure 6(a)). These results are also in accordance with the XRD analysis. A significant proportion of the NPs in the LPLA sample is considered to be transformed into the fct phase, because the Debye–Scherrer ring of 110 is distinctly closed as shown in the inset of figure 6(b). Hence, we conclude that the crystalline structure was successfully transformed into the ordered fct phase, without severe coalescence by the 1 mm spot beam irradiation. In addition, the composition of the 1 mm spot LPLA sample is $Fe_{57}Pt_{43}$, determined by ICP-AES, which is identical to that of the as-synthesized sample.

Finally, regarding the magnetizing properties of laser annealed samples, figure 7 shows the magnetization curves of the FA, SPLA and 1 mm spot LPLA samples. The as-synthesized sample showed superparamagnetism (data not shown). In contrast, the FA sample (solid curve in figure 7) exhibited ferromagnetism, showing coercivity of 6 kOe. The 1 mm spot LPLA sample (open circles) was superparamagnetic despite the existence of fct phase. This would be due to the significant suppression of coalescence and the resulting small size of NPs as mentioned above [10]. In the case of FePt crystallites, the superparamagnetic size limit is estimated to be about 3 nm [21, 27]. Namely, fct-FePt NPs exhibit paramagnetic behaviour when their size is smaller than 3 nm at room temperature. Hence, our results are consistent with these previous studies. To obtain isolated 'ferromagnetic' fct-FePt NPs, one should prepare monodispersed NPs larger than the critical size (3 nm) at the stage of synthesis. On the other hand, the SPLA sample clearly exhibited a calabash-shaped magnetization curve (filled circles), suggesting the existence of a mixture of the ferromagnetic fct phase and the superparamagnetic fcc phase. However, the coercivity of 1 kOe observed in the SPLA sample is much smaller than that of the FA sample. In the case of SPLA, the coalescence of NPs might proceed more significantly than LPLA. Thus, the magnetic domain size became larger than the critical size showing ferromagnetism. Slight variation in the XRD pattern and the distorted shape of the magnetic hysteresis loop suggest strong inhomogeneity in the film. In consequence, we confirmed that laser annealing can transform FePt NPs from disordered fcc into chemically ordered fct phase. By utilizing SPLA, the patterning of magnetic thin films, which has usually

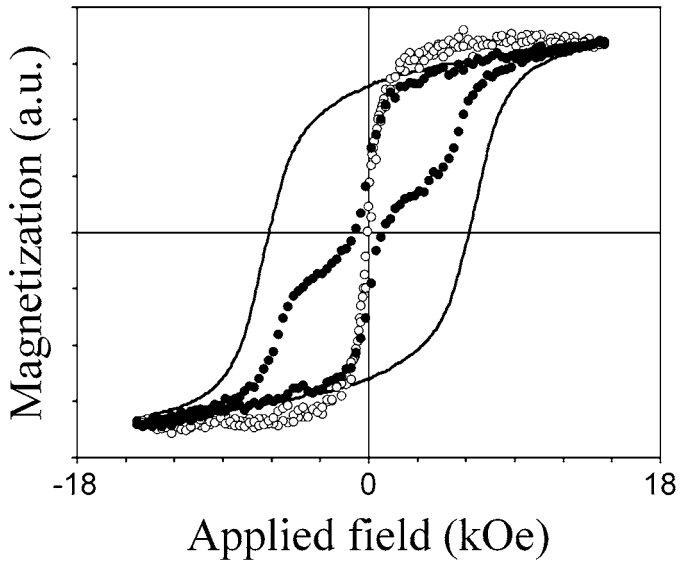

Figure 7. Room-temperature magnetization curves of FePt NPs. The solid curve represents the hysteresis loop of the FA sample. Open and filled circles represent the magnetization curves of the 1 mm spot LPLA and SPLA samples, respectively.

been carried out by lithographic techniques, like ion beam irradiation [28], can be achieved utilizing the easy-to-use and inexpensive laser scanning method. Very recently, Sun and co-workers have reported direct thermal patterning of self-assembled FePt NPs utilizing laser irradiation [29]. Specifically, using laser heating they have fabricated ferromagnetic FePt NP array patterns with 800 nm pitch. In their case, however, the phase transformation of FePt NPs from fcc into fct was conducted by conventional thermal annealing in N_2 atmosphere after the laser patterning process. In short, the laser heating did not change the crystal structure of NPs because a maximum temperature during laser irradiation was insufficient. In contrast, in our case, the phase transformation was promoted by laser irradiation without any additional heat treatment.

4. Conclusion

Chemically disordered fcc-FePt NPs synthesized by the colloid–chemical route were transformed into ordered fct-FePt NPs by utilizing the pulsed laser annealing technique. A granular film and hexane dispersions of fcc-FePt NPs were irradiated by the pulsed laser beam of the third-harmonic wave of a Nd:YAG laser with a 5 ns pulse width. In the case of the granular film, the coercivity of 1 kOe was achieved with a slight variation of the XRD pattern by the irradiation of a 2 mm spot beam. By utilizing this technique, the patterning of magnetic thin films can be achieved. On the other hand, the dispersion sample exhibited superparamagnetism because the NPs were smaller than the critical size, although the crystalline structure was successfully transformed into ordered fct phase, without severe coalescence by 1 mm spot beam irradiation. This result suggests that the preparation of monodispersed NPs larger than the critical size at the stage of synthesis is necessary to obtain isolated ‘ferromagnetic’ FePt NPs by using laser annealing as a future issue.

Acknowledgments

We are grateful to Dr Y Sasaki (Centre for Analytical Chemistry and Science, MCRC, Inc.) for assistance with the laser annealing experiments and Dr H Matsumoto and Dr M Takashima (Centre for Analytical Chemistry and Science, MCRC, Inc.) for the high-resolution TEM observations. We also thank H Asatani, M Yoneyama and K Kowalczyk for carefully reading the manuscript.

References

[1] Dormann J L and Fiorani D 1995 *J. Magn. Magn. Mater.* **140** 415
[2] Pfannes H D, Mijovilovich A, Magalhaes-Paniago R and Paniago R 2000 *Phys. Rev.* B **62** 3372
[3] Sun S, Murray C B, Weller D, Folks L and Moser A 2000 *Science* **287** 1989
[4] Sun S, Fullerton E E, Weller D and Murray C B 2001 *IEEE Trans. Magn.* **37** 1239
[5] Weller D, Sun S, Murray C B, Folks L and Moser A 2001 *IEEE Trans. Magn.* **37** 2185
[6] Robach O, Quiros C, Valvidares S M, Walker C J and Ferrer S 2003 *J. Magn. Magn. Mater.* **264** 202
[7] Hsiao H H, Panda R N, Shih J C and Chin T S 2003 *J. Appl. Phys.* **91** 3145
[8] Jeyadevan B, Hobo A, Urakawa K, Chinnasamy C N, Shinoda K and Tohji K 2003 *J. Appl. Phys.* **93** 7574
[9] Kang S S, Nikles D E and Harrell J W 2003 *J. Appl. Phys.* **93** 7178
[10] Yu A C C, Mizuno M, Sasaki Y, Inoue M, Kondo H, Ohta I, Djayaprawira D and Takahashi M 2003 *Appl. Phys. Lett.* **82** 4352
[11] Enpuku K, Kuroda D, Yang T Q and Yoshinaga K 2003 *IEEE Trans. Appl. Supercond.* **13** 371
[12] Plank C, Schillinger U, Scherer F, Bergemann C, Remy J S, Krotz F, Anton M, Lausier J and Rosenecker J 2003 *Biol. Chem.* **384** 737
[13] Mazaleyrat F and Varga L K 2000 *J. Magn. Magn. Mater.* **215** 253
[14] Jeyadevan B, Urakwawa K, Hobo A, Chinnasamy N, Shinoda K, Tohji K, Djayaprawira D, Tsunoda M and Takahashi M 2003 *Japan. J. Appl. Phys.* 2 **42** L350
[15] Bell A E 1979 *RCA Rev.* **40** 295
[16] Brotherton S D 1995 *Semicond. Sci. Technol.* **10** 721
[17] Stepanov A L and Hole D E 2002 *Surf. Coat. Technol.* **158/159** 526
[18] Takami A, Kurita H and Koda S 1999 *J. Phys. Chem.* B **103** 1226
[19] Fujiwara H, Yanagida S and Kamat P V 1999 *J. Phys. Chem.* B **103** 2589
[20] White C W, Withrow S P, Sorge K D, Meldrum A, Budai J D, Thompson J R and Boatner L A 2003 *J. Appl. Phys.* **93** 5656
[21] Huang Y H, Zhang Y, Hadjipanayis G C and Weller D 2003 *J. Appl. Phys.* **93** 7172
[22] Vedantam T S, Liu J P, Zeng H and Sun S 2003 *J. Appl. Phys.* **93** 7184
[23] Stoyanov S, Huang Y, Zhang Y, Skumryev V, Hadjipanayis G C and Weller D 2003 *J. Appl. Phys.* **93** 7190
[24] Huang J Y 1999 *Acta Mater.* **47** 1801
[25] Robineau M and Zins D 1995 *Ann. Chim., Sci. Mater.* **20** 327
[26] Nair P S, Radhakrishnan T R, Revaprasadu N, Kolawole G and O'Brien P 2002 *J. Mater. Chem.* **12** 2722
[27] Watanabe M, Nakayama T, Watanabe K, Hirayama T and Tonomura A 1996 *Mater. Trans. JIM* **37** 489
[28] Terris B D, Weller D, Folks L, Baglin J E E, Kellock A J, Rothuizen H and Vettiger P 2000 *J. Appl. Phys.* **87** 7004
[29] Hamann H F, Woods S I and Sun S 2003 *Nano Lett.* **3** 1643